Multifractal analysis of evolving noise associated with unstable plastic flow

M. A. Lebyodkin[1,2,*] and T. A. Lebedkina[1,†]
[1]*Institute of Solid State Physics, Russian Academy of Sciences, 142432 Chernogolovka, Russia*
[2]*Laboratoire de Physique des Matériaux, UMR CNRS-UHP-INPL NO. 7556, Ecole des Mines de Nancy, Parc de Saurupt, 54042 Nancy cedex, France*
(Received 16 November 2005; published 10 March 2006)

Plastic flow instability attracts increasing interest as a self-organization phenomenon showing various dynamical regimes, including deterministic chaos and self-organized criticality. The analysis of the associated nonrandom noise—drastic jumps of the mechanical stress—however, confronts the variation of the noise average parameters due to the evolution of the dislocation microstructure. The present paper examines some limitations of the multifractal approach to the study of the evolving noise. The applicability of the multifractal analysis to practical situations is proven using the example of discontinuous deformation curves observed under conditions of the Portevin-Le Châtelier effect in an AlMg alloy, as well as model signals generated by stretching multifractal Cantor sets. It is found that the smooth trends in the stress serration parameters may narrow the range of the scale invariant behavior associated with the multifractal structure, but do not essentially mask it.

DOI: 10.1103/PhysRevE.73.036114 PACS number(s): 62.20.Fe, 05.45.Tp, 05.45.Df, 83.60.Wc

I. INTRODUCTION

One of the well-known manifestations of plastic instability is the emergence of serrations on the deformation curves due to the repetitive occurrence of spatially localized plastic flow with very high strain rates, which may be caused by various microscopic mechanisms [1,2]. Recent studies showed that the complex spatiotemporal behavior associated with plastic instability is a consequence of the self-organization of dislocations interacting with each other and with other crystal defects. Using various methods of analysis of discrete time series, a rich behavior was found in a number of works (see [3–14], and references therein) under conditions of the Portevin-Le Châtelier (PLC) effect, an unstable plastic flow related to the generation and propagation of localized deformation bands in dilute alloys [15]. In particular, dynamical chaos [16] characteristic of nonlinear systems with a small number of degrees of freedom was found in [4–6,8]. At the same time, self-organized criticality predicted for extended systems [17] was detected in [3,7–9]. It was proven that these two distinct dynamical regimes may occur in the same material under different experimental conditions and that the corresponding transition is related to a transition from localized to propagating deformation bands with an increasing strain rate [8,11]. Moreover, there are indications that a similar dynamical behavior may show up for other microscopic mechanisms of plastic instability [18–21].

The multiscale nature of the observed behavior suggested the use of the multifractal analysis [22] of serrated deformation curves as a general framework for the plastic instability investigation [11,13]. It was found that the deformation curves often show a multifractal structure in a limited scaling range depending on the experimental conditions. In particular, a drastic widening of the multifractal spectrum was observed at the localization-propagation transition mentioned above [11]. Such a behavior is similar to the multifractality predicted for the Anderson transition from localized to delocalized electron wave functions [23]. This adds to the interest of plastic instability, which can be seen as representative of a broader class of phenomena.

However, the investigation of the unstable plastic flow is impeded by the evolution of the defect microstructure during deformation, which leads to the strain hardening of the material together with an alteration of the average parameters of the stress fluctuations. The general question of the robustness of the multifractal structure of real signals with regard to their unsteadiness is thus addressed in the present paper, using the example of the PLC effect. It is shown that the noise evolution narrows the scaling extension but does not essentially alter the multifractal structure in practical situations. It is then possible to avoid arbitrary hypotheses in the signal preprocessing aimed at removing the undesirable trend. The results obtained are confirmed on model structures generated by deliberately distorting multifractal Cantor sets.

The outline of the paper is as follows. Section II describes the microscopic mechanism of the PLC effect and some peculiar features of the macroscopic behavior of serrated deformation curves. Experimental details and the numerical technique used for the data analysis are presented in Sec. III. In Sec. IV, the results of the multifractal analysis of the experimental data and the model Cantor sets are discussed. The conclusions are outlined in Sec. V.

II. THE PORTEVIN-LE CHATELIER EFFECT

The dynamical nature of the PLC instability can be qualitatively understood by considering the strain rate sensitivity (SRS) of the flow stress, which plays a similar role in the plasticity problems to that of the resistance in electric cir-

*Electronic addresses: mikhail.lebedkin@mines.inpl-nancy.fr; lebedkin@issp.ac.ru
†Electronic address: tlebyod@issp.ac.ru

cuits. An increase in the strain rate $\dot{\varepsilon}$ requires a decrease in the waiting time of dislocations at obstacles to be overcome by thermal activation. This is ensured by a higher flow stress σ, thus leading to an ascending $\sigma(\dot{\varepsilon})$ dependence and a positive SRS. On the other hand, the segregation of solute atoms at dislocations during the waiting time (dynamical strain aging) results in additional dislocation pinning, the strength of which follows an opposite dependence: it becomes weaker with increasing $\dot{\varepsilon}$ because less time is available for aging. The competition of these two trends gives rise to a region of strain rate values where the SRS is negative, the overall dependence acquiring an N shape. During a test under a constant imposed strain rate $\dot{\epsilon}_a$ within the negative-slope range, this brings to the relaxation-oscillation type of instability [24], i.e., a cyclic behavior comprising $\dot{\varepsilon}$ jumps between the slow and the fast positive-slope branches of the N shaped curve, which are transferred into drastic σ falls by the elastic reaction of the deforming machine.

This qualitative consideration assumes that all dislocations behave equally. However, the strain heterogeneity in real samples depends on both internal factors, such as the material microstructure and composition, and on the experimental conditions, including the strain rate, the temperature, and the test scheme. This leads to a great variety of serration patterns [1]. Therefore, the analysis of the stress fluctuations is expected to shed light on the collective dynamics of dislocations under various conditions.

Such an analysis is complicated by the strain hardening which occurs at a slower time scale corresponding to the overall test duration. This is illustrated in Fig. 1(a) that shows a deformation curve of an AlMg polycrystal exhibiting the PLC effect. It can be seen that the plastic flow requires a gradually increasing average stress level. This strain hardening would not prevent us from analyzing statistical properties of stress fluctuations if it did not influence on their averaged parameters. However, such constancy is usually not the case. One of the consequences of strain hardening is a smooth alteration of the average stress jump depth, as can be readily seen in Fig. 1(a). This is usually easily taken into account with the aid of the following procedure. First, a short enough portion of the nearly stabilized deformation curve at the late deformation stage, corresponding to the least strain hardening rate, is allotted for the analysis. This portion should be long enough to provide a significant statistical data sample. For this reason, the remaining effect of the strain hardening on the span of the stress oscillations is removed by normalizing the selected portion. Various normalization procedures adapted to a specific analysis were described, e.g., in [3–9,11]. In particular, since the current stress level and the jump scale are both related to the microstructure state, this allows for a physically based normalization of the deformation curve with regard to the average trend $\Delta\sigma(t)$. Providing that the average interjump intervals do not noticeably change, the normalized time series may be considered stationary and analyzed.

The possible evolution of the interjump intervals has never been discussed in this concern, which is partly due to the observation of a weaker effect of strain hardening on the jump frequency in comparison with the influence on their size. However, many authors reported significant frequency changes in the course of deformation (e.g., [25]). Apparently, the nonconstancy of the intervals is more difficult to take into account. To begin with, there are no obvious physical grounds for the time reconstruction called to mimic a stationary behavior. At first sight, the plastic strain ϵ might be used instead of time, which may not be a proper variable accounting for the microstructure evolution. However, the strain dependence of the strain increments accumulated between stress jumps shows similar qualitative trends as those observed for the time delays. Furthermore, the time reconstruction would require more sophisticated numerical procedures than the normalization of the jump amplitudes. Indeed, when the entire time series and not only the series of stress jumps are to be analyzed, this would imply a step-by-step reconstruction of the deformation curve and, therefore, an accumulation of numerical errors. In this concern, the present paper aims at evaluating the influence of the slow evolution on the multifractal analysis of the original deformation curves, as well as the workability of numerical procedures suggested for the curve reconstruction.

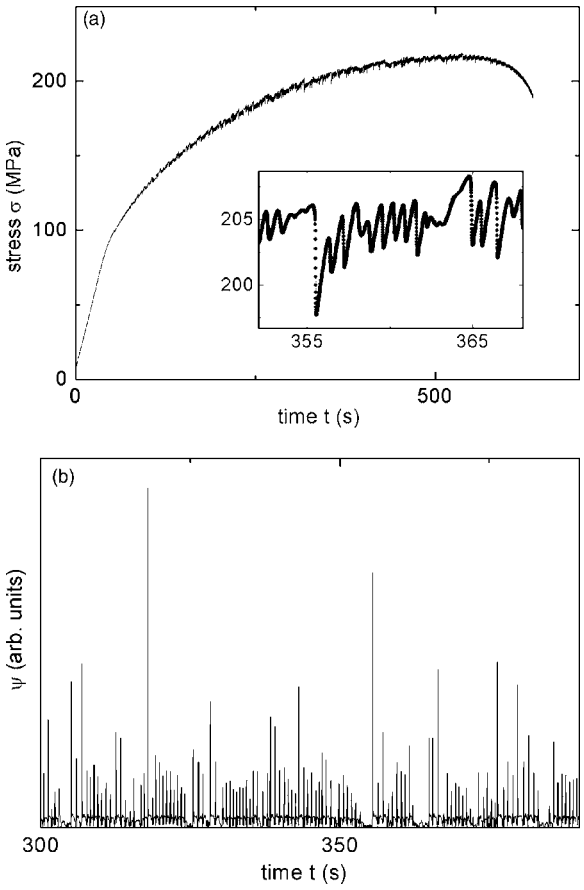

FIG. 1. Example of a stress-time curve $\sigma(t)$ of an AlMg polycrystalline sample deformed at a strain rate of 6×10^{-4} s^{-1} and (b) the corresponding plot of the absolute value of the derivative $\psi(t)=|d\sigma/dt|$. The inset in (a) shows a rescaled portion of the deformation curve.

III. METHODOLOGY

The study included two complementary approaches. First, the multifractal properties of the original and reconstructed

time series were compared using deformation curves recorded at different strain rates in order to provide a basis for contrasting physical effects with numerical artifacts. The second approach was based on the similarity between the nonuniform Cantor sets [26] and the sequences of stress drop amplitudes extracted from deformation curves. With this similarity in view, Cantor sets with known multifractal spectra were deliberately distorted to mimic gradual changes in the jump size or frequency along the deformation curve. The spectra calculated for the initial Cantor set and for its distorted version were then compared.

The mechanical tests were carried out with a typical setup for the observation of the PLC instability (see, e.g., [3]). Flat polycrystalline specimens of a Al-3 at. % Mg alloy, with a gauge length, width, and thickness of 25, 6.5, and 2.0 mm, respectively, were annealed at 400 °C for 2 h to provide a uniform solute concentration, quenched in water, and immediately deformed at room temperature with a constant strain rate in the range from 7×10^{-6} s^{-1} to 7×10^{-3} s^{-1}. The stress was recorded at a sampling rate of 2–500 Hz, depending on the strain rate value so that the number of data points available for the multifractal analysis was typically around ten thousand. Special attention was paid to the sufficient sampling of stress jumps [see the inset in Fig. 1(a)]. In addition, the persistency of the analysis was checked by thinning out the original data sets. It was proven that even keeping only every fourth data point did not change the results of the data processing.

The multifractal analysis is based on the hypothesis that the natural complexity often arises from a self-similar, or scale-invariant, behavior, rather than from randomness or from superposition of multiple oscillations. In particular, both the deterministic chaos and the self-organized criticality are related to self-similarity. Since the multifractal analysis was introduced in [23], it has been reviewed in several books (see, e.g., [26]). Its application to discontinuous deformation curves was described in detail in [11,13]. In the present report, we only discuss some relevant features of the procedure employed.

Following the approach proposed in the previous investigations of the multifractal structure of deformation curves [11], we analyzed the absolute value of the finite difference approximant $\psi_j(t_j)$ of the time derivative of stress $|d\sigma/dt|$, i.e., a variable reflecting the plastic flow bursts [see Fig. 1(b)]. Such an approach was also justified in [13], where the results were compared to the multifractal characteristics obtained using stress increment series $|\sigma_{j+1}-\sigma_j|$. Both kinds of signals provided close results robust with respect to the experimental noise.

The $\psi_j(t_j)$ time series were constructed using three kinds of data files: portions of the original deformation curves, the same portions after leveling off the average stress jump size, and, finally, after additional reconstruction allowing for the variable jump frequency, as described below. Recalculation of the initial data files was based on the apparent linear trends in the evolution of both the jump size and interjump intervals (see Sec. IV). The jump size variation was eliminated by normalization using a linear regression fit through the $\Delta\sigma(t)$ dependence. Herewith, the slow strain hardening component was preliminary removed by subtracting a polynomial fit of the deformation curve. It should be noted that a more delicate moving average procedure was proposed in [11]. The coarser averaging applied in the present paper was aimed at minimizing the influence of the averaging method on the discontinuity studied. The constant jump frequency was provided by a gradual rescaling of the sampling intervals dt in proportion to the linear regression fit $f(t)$ through the time dependence $\Delta t(t)$ of the interjump intervals

$$dt_j^* = t_{j+1}^* - t_j^* = \frac{dt}{f(t_j)}, \tag{1}$$

where j is the serial number of the data point.

The multifractal spectra were calculated by the box-counting fixed-size technique [27]. For this, the time interval selected for the analysis was covered with a grid with the box length δt that was varied as a power of 2. The starting point for the covering was chosen at random, and the estimate of the fractal dimensions was obtained by averaging over ten trials. The probability measure $\mu_i(\delta t)$ was calculated as a normalized sum of ψ magnitudes in the ith interval δt:

$$\mu_i(\delta t) = \sum_{k=1}^{n} \psi_k \Big/ \sum_{j=1}^{N} \psi_j, \tag{2}$$

where N is the whole number of data points in the sample and n the number of points in the ith interval. The qth moments of the measure of a multifractal set should obey the following scaling laws in the limit of $\delta t\to 0$ (in practice, the scaling is limited by the sampling time):

$$Z_q(\delta t) = \sum_i \mu_i^q \sim \delta t^{(q-1)D(q)} \quad (q \neq 1),$$

$$Z_1(\delta t) = \sum_i \mu_i \ln(\mu_i) \sim D(1)\ln\delta t. \tag{3}$$

As q is varied from $q=-\infty$ to $q=\infty$, different μ values, associated with different data subsets, consecutively become dominant in the above sums. The corresponding scaling dependences thus determine a continuous spectrum $D(q)$ of generalized dimensions that provide a quantitative description of the data complexity. Herewith, Z_0 simply gives the number of boxes with nonzero measure, so that $D(0)$ is the fractal dimension of the geometrical support on which the measure is distributed [22].

The following examples describe some typical situations. In the trivial case of a constant signal, $\psi_j(t_j)=\text{const}$, which homogeneously fills the space, all D values are equal to unity. This would also come out for a random or a periodic signal in a range of box sizes exceeding a certain characteristic time (e.g., the oscillation period). A clustering of events may produce self-similar fractal structures. Among those, the uniform fractals are also characterized by a unique fractal dimension, which depends on the clustering degree and, therefore, reflects the underlying structure. Finally, the description of a heterogeneous multifractal object requires a set of scaling indices. In particular, this means that their range may be considered as a degree of the structure heterogeneity.

It should be noted that the use of the whole set of experimental data points $\psi_j(t_j)$ imposes $D(0)\approx 1$. Indeed, the geometrical support of the corresponding measure is the whole time interval, with the exception of a small number of points where $\psi_j(t_j)=0$. Thus, the intermittent nature of the jump generation (nucleation of the PLC bands) does not directly come out in this kind of analysis. In return, the use of the $\psi_j(t_j)$ series instead of a series of stress jumps makes it possible to avoid the arbitrariness associated with discrimination of small jumps against the unknown measurement noise.

We also calculated singularity spectra $f(\alpha)$ that allow for a direct physical interpretation [22]. Namely, the local value of the measure obeys a scaling law $\mu_i(\delta t)\sim \delta t^{\alpha}$, and $f(\alpha)$ is the fractal dimension of the support of the subset associated with the same α. The value of α has a clear physical meaning: it indicates the local singularity of the signal. Indeed, the measure density $\mu_i/\delta t\sim \delta t^{\alpha-1}$ diverges if $\alpha<1$. It was proven that the two kinds of the description are equivalent: the functions $f(\alpha)$ and $D(q)$ are related by the Legendre transformation [22]. In particular, the range of the singularity strength α is confined by the saturation levels of the generalized dimensions: $\alpha_{min}=D(\infty)$ and $\alpha_{max}=D(-\infty)$.

The singularity spectrum was calculated using scaling relationships for a modified measure, $\tilde{\mu}_i(\delta t,q)=\mu_i^q/\Sigma_j\mu_j^q$, as proposed in [28]:

$$\Sigma_\alpha(\delta t,q)=\sum_i \tilde{\mu}_i(\delta t,q)\ln\mu_i(\delta t)\sim \alpha(q)\ln\delta t,$$

$$\Sigma_f(\delta t,q)=\sum_i \tilde{\mu}_i(\delta t,q)\ln\tilde{\mu}_i(\delta t,q)\sim f(q)\ln\delta t. \qquad (4)$$

The test nonuniform Cantor sets were treated in the same way as the experimental $\psi_j(t_j)$ series. To mimic the stress jump frequency alteration with strain hardening, the Cantor set was proportionally stretched (or compressed) according to Eq. (1), where the time variable should be replaced with the coordinate l, and using the function

$$f(l)=1+\beta\frac{l}{L}. \qquad (5)$$

Here, L is the overall length of the Cantor set support, and β is the stretching factor. In addition, the effect of stretching along the ordinate axis, which corresponds to the stress jump amplitudes, was also tested using the same proportionality function.

IV. RESULTS AND DISCUSSION

A. Multifractal structure of experimental curves

Figure 2 represents time dependences of the stress jump amplitudes and interjump intervals for the deformation curve shown in Fig. 1 ($\dot{\varepsilon}_a=6\times10^{-4}$ s^{-1}). Such dependences are typical of the range of strain rates $\dot{\varepsilon}_a$ below 10^{-3} s^{-1}, within which the deformation curves are reminiscent of relaxation oscillations and reveal characteristic amplitude and frequency scales that may evolve during deformation. The

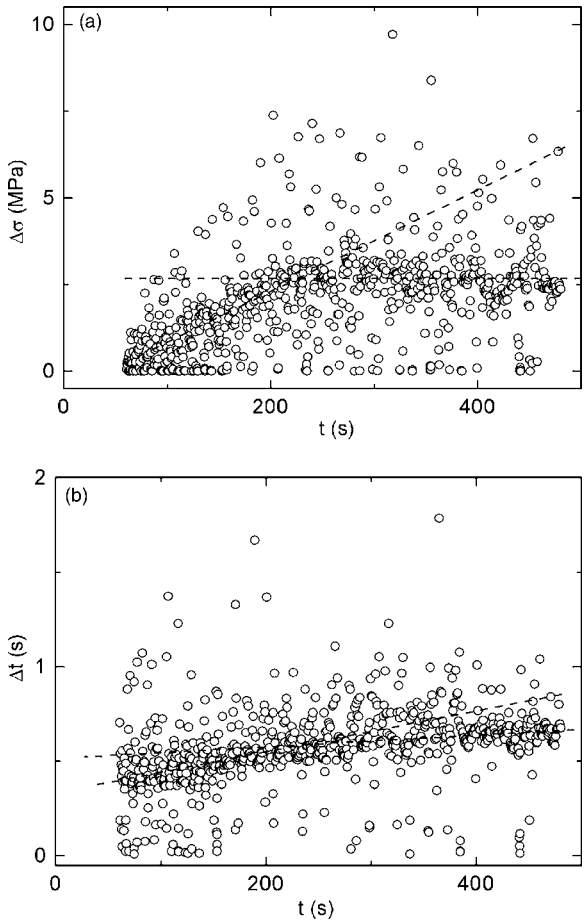

FIG. 2. Time dependences of (a) the stress jump size $\Delta\sigma$ and (b) intervals Δt between the neighboring jumps. The dashed lines show regions with different values of the average rate of growth of the jump parameters.

curves display two distinct portions that on average behave in a roughly linear manner and are characterized by different slopes. The initial stage (ϵ below approximately 5–8 %), hereafter referred to as a transient behavior, corresponds to a strong hardening rate and fast growth of both $\Delta\sigma$ and Δt. The transient behavior is followed by a stage close to a hardening saturation, which is thought to reflect a quasistationary dynamical behavior and is usually studied. Indeed, the visual appearance of serrations becomes more regular and the corresponding data in Fig. 2 display almost no time dependence of $\Delta\sigma$ and only a slight increase in Δt. However, considerably stronger dependences of the jump parameters at the saturation stage, either ascending or descending, were observed, also (see also [25]). In some cases, the changes corresponded to a stretching factor $|\beta|$ up to 0.5 [see Eq. (5)]. Therefore, neither stage can, in general, be saved from taking care of the effects caused by the signal variation with the strain hardening. In the present work, the multifractal characteristics were calculated for both deformation stages. The analysis of the transient portion, alongside with providing an opportunity to evaluate the multifractal technique in the most unfavorable conditions, gives a handle to the study of the transient behavior, almost unexplored for the time present.

For higher $\dot{\varepsilon}_a$ values, the average stress jump parameters were practically constant except for a short initial stage that

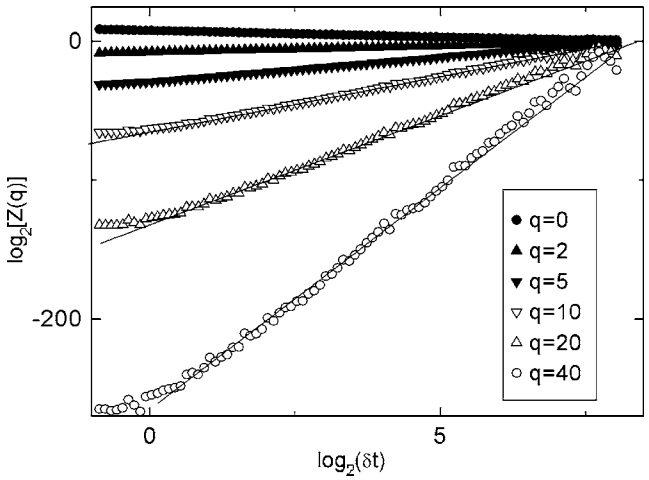

FIG. 3. Dependences of the qth moments Z_q of the probability measure on the grid box length δt [see Eq. (3); arbitrary units] for a time series obtained upon eliminating the growth of the stress jump size at the transient stage of the deformation curve ($\dot{\epsilon}_a=6\times10^{-4}$ s^{-1}).

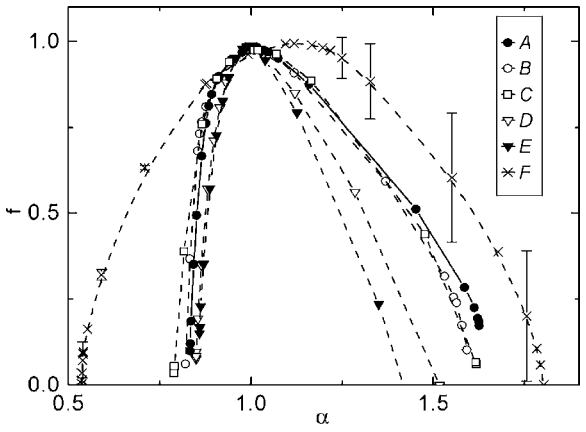

FIG. 4. Examples of the singularity spectra for $\dot{\varepsilon}_a=6\times10^{-4}$ s^{-1} (curves $A-E$) and $\dot{\varepsilon}_a=6\times10^{-3}$ s^{-1} (curve F). The data for the lower strain rate were separately processed at the transient stage (curves $A-C$) and the quasistationary stage (curves D and E). The figure illustrates the effect of the evolution of the stress serrations: the $\psi_j(t_j)$ series were calculated for the original stress-time curves (curves A and F), after normalization of the stress jump amplitudes (curves B and D) and after additional time reconstruction (curves C and E). Error bars (only shown for curve F in order to avoid overcharging of the figure) show that the scaling indices are well defined in the positive q range corresponding to the left ascending branches of the spectra.

was cutoff. This strain rate range corresponds to very irregular deformation curves with a jump statistics that progressively acquires a power-law shape when the strain rate is increased (see, e. g., [1] for the serration type nomenclature). Such a behavior, characterized by the disappearance of inherent event scales, is akin to self-organized criticality [17]. In this case, only one kind of $\psi_j(t_j)$ time series, namely, the time derivative of the original deformation curve was analyzed.

The multifractal structure was revealed for most of experimental curves in some scaling intervals. Figure 3 presents an example of the scaling dependence (3) for the transient stage ($t\leqslant220$ s) of the deformation curve shown in Fig. 1. The corresponding $\psi_j(t_j)$ series was obtained by leveling off the stress jump size. It can be recognized that scaling may be clearly detected for these data in spite of the time dependence of the interjump intervals, which remained intact upon the curve preprocessing.

The influence of various types of the deformation curve reconstruction on the corresponding multifractal structure is illustrated in Fig. 4. It compares the singularity spectra $f(\alpha)$ calculated using three kinds of time series for both the transient (curves A-C) and quasistationary (curves D and E) deformation at $\dot{\epsilon}_a=6\times10^{-4}$ s^{-1}. Also shown is a spectrum obtained for a sample deformed at a higher strain rate, $\dot{\epsilon}_a=6\times10^{-3}$ s^{-1} (curve F). Figure 4 is representative of some general features relevant to all specimens. First of all, the results for positive q values (left parts of the singularity spectra) are quite close for the original and reconstructed time series. For example, the horizontal shift between curves A (original deformation curve) and C (both the jump amplitudes and interjump intervals were leveled off) comprises approximately 0.045 ± 0.002 for $\alpha(40)\approx\alpha_{min}=D(\infty)$ and 0.007 ± 0.0003 for $\alpha(0)$. Here, the average slopes of the corresponding scaling dependences [see Eq. (4)] and the standard deviations were estimated by the least squares method. In the whole set of experiments, the maximum change in α_{min} upon any kind of reconstruction of the transient stage did not exceed 0.05. This value is considerably smaller than the shifts observed upon variation of the experimental conditions, which leads to qualitative changes in the shape of the deformation curves, indicative of transitions between different dynamical regimes of the PLC effect. Indeed, the difference between α_{min} values measured for curve F (high strain rate) and for the group of curves A-E (lower strain rate) is approximately 0.3, i.e., six times the variation caused by reconstruction. Moreover, the examples in Fig. 4 show that reconstruction of the quasistationary stage left the multifractal characteristics practically uninfluenced. For instance, no noticeable shift can be detected between curves D (jump size normalization) and E (full reconstruction). It can be seen that $f(40)$ was the only parameter manifesting strong alterations upon reconstruction. However, these changes may not be considered significant. As a matter of fact, the extreme values $f(\pm\infty)$ cannot be drawn from experimental data with a high certainty because of the infinite slopes of the singularity spectrum at $q=\pm\infty$ [22]. Indeed, the vertical error bars shown for several data points in Fig. 4 are negligible at the top of the spectra and quickly grow towards the edges. The level of uncertainty is similar for different curves in Fig. 4 and is only shown for the separately lying curve F in order to avoid overcharging of the plot. For the spectra presented in Fig. 4, the changes in the estimate of the dimension $f(40)$ after reconstruction were inferior to approximately 0.08; this value did not exceed the standard deviation estimate (from 0.09 to 0.15 for various curves plotted in the figure).

It may be concluded that the unsteadiness of the noise related to the PLC effect does not crucially hide its multifractal structure for $q\geqslant0$. The data of Fig. 4 also show that

the results for negative q values (right branches of the singularity spectra) are rather sensitive to reconstruction. Moreover, the right branches of curves D, E, and F drop to the nonphysical region: $f(\alpha)<0$. This is related to the fact that the negative q values correspond to the lowest μ_i and, therefore, the scaling is evaluated on a poor statistical basis of the most rarified measure (cf. large error bars in the corresponding q range). In this case, a fixed-mass technique, which forces accumulation of sufficient statistical samples, may give better results [27]. In the present work, its application only slightly improved the calculation results. This is obviously due to a rather poor overall statistics of the plastic instability events accumulated before the specimen failure. Thus, it is advisable to confine the multifractal analysis of real deformation curves to the range of $q \geqslant 0$.

Whereas the reconstruction of deformation curves almost did not change the slopes of the scaling dependences, it enhanced the scaling range in some cases. The scaling range found for the original curves typically comprised 1 to 1.5 orders of magnitude of δt. Such a short range may be due to a number of factors, either physical (see [29] for the discussion of the intrinsic cutoffs in empirical fractals) or related to the measurement imperfection: the strain hardening effect addressed here, the superposition of various microscopic mechanisms of plastic flow, the finite specimen size, the inherent deficit of the instability events because of the final specimen fracture, the instrumental noise, or the limited experimental resolution. It was found that the extension of the scaling range sometimes reached half a decade upon the curve preprocessing, which justifies application of the reconstruction. However, it should be kept in mind that the physical grounds for the time reconstruction are unclear. As a compromise, the following procedure may be proposed. To avoid physical arbitrariness and numerical errors, the signal preprocessing should be limited to leveling off the stress drop size. If no scaling is found, a time reconstruction may be undertaken in order either to corroborate the nonfractal nature of the deformation curve or to reveal its possible multifractal structure.

It should be noted that these results also show the necessity of an extreme caution in the analysis of experimental data. Indeed, reconstruction of the transient deformation stage was accompanied by detectable changes in the multifractal spectra. This imposes a great care when interpreting small variations of the fractal dimensions, often reported in literature.

Interpretation of the multifractal structure of deformation curves, as well as its limitations, goes beyond the scope of the present paper. Some successful attempts of the physical explanation, which made it possible to judge on the correlation of the motion of dislocations, were reported in the previous works [11,13]. Nevertheless, one aspect is worth underlining here. Namely, the closeness of the multifractal characteristics found for the transient and quasistationary deformation stages testifies that the dislocation processes involved in the PLC effect remained qualitatively the same over the entire deformation curve in the tests performed. On the other hand, this shows that the multifractal analysis is a useful tool to distinguish essential dynamical features of the deformation curves. It should be noted that the observed uniqueness is not a general property of the PLC effect that manifests a great variety of behaviors. In particular, qualitative changes in the deformation curve shape, which bear witness to the transitions between different dynamical regimes, may occur in the course of deformation without need to change the strain rate or temperature [3,9,30].

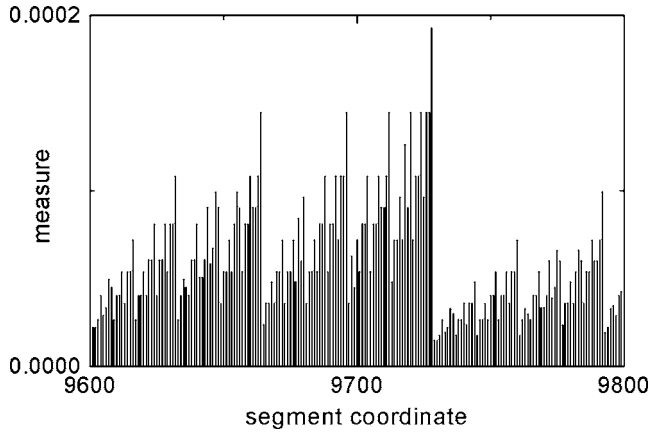

FIG. 5. Measure for a multifractal Cantor set distributed on an interval [0;16384].

B. Influence of stretching of multifractal Cantor sets

The reason for the robustness of the multifractal structure of the experimental time series becomes clear when the effect of distortion of multifractal Cantor sets is considered. The Cantor sets were constructed following a multiplicative procedure of iterated division of an interval into i pieces in such a way that the size of the ith peace is reduced by a factors l_i and the measure ascribed to the piece is reduced by a factor p_i in each iteration step [26,27].

Figure 5 presents an example of a multifractal set constructed using the rescaling factors $l_i=\frac{1}{4}$ ($i=1$ to 4), $p_1=\frac{1}{6}$, $p_2=p_3=\frac{1}{4}$, and $p_4=\frac{1}{3}$. The corresponding scaling dependences for two q values are shown in Fig. 6 and are compared to the dependences for the same set stretched in the horizontal direction. To illustrate the effect of stretching, an unrealistically high value of $\beta=3$ [see Eq. (5)] was deliberately chosen. It can be seen that even for such a high β value, stretching only influences on the large-scale part of the dependences. The deviation becomes more abrupt when q is increased. However, the inflection point does not move with changing q, so that the multifractal characteristics can be conveniently determined. It can be seen that in the limit $\delta t \rightarrow 0$, the scaling dependences have approximately the same slope before and after stretching and, therefore, the multifractal spectra almost coincide for both sets for $q \geqslant 0$ (Fig. 7). Curve C in Fig. 7 presents the multifractal spectrum of the Cantor set that was stretched in both the horizontal and normal directions, which corresponds to increasing both the stress jump amplitudes and interjump intervals. Here, the same stretching factor was used for both axes. It can be recognized that the multifractal structure persists at $q \geqslant 0$ in this case, too. Such endurance seems to be a consequence of

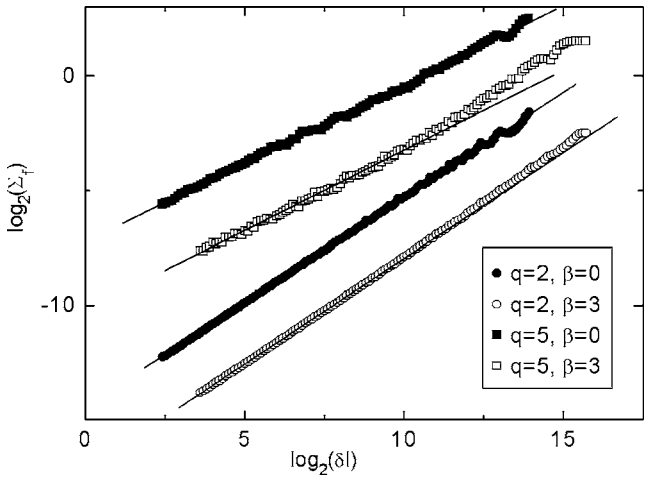

FIG. 6. Examples of scaling dependences used to extract the fractal dimension $f(q)$ for an original multifractal set ($\beta=0$) and for the same set after stretching of the intervals between segments in proportion to the segment coordinate with the stretching factor $\beta=3$ [see Eq. (5)]. Σ_f is given by Eq. (4), δl is the grid size (arb. units).

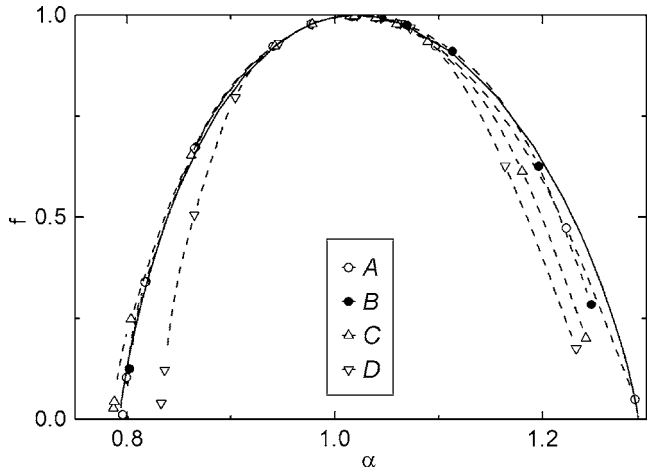

FIG. 7. Singularity spectra calculated for the multifractal set. The solid line shows the analytical dependence. *A*, spectrum calculated for the original set; *B*, results of the calculation after stretching in the horizontal direction ($\beta=3$); *C*, stretching in both horizontal and vertical directions ($\beta=3$); and *D*, horizontal stretching with $\beta=10$.

the scale invariance: when the signal is stretched or compressed, the new elements replacing the old ones at a given scale level have the same multifractal structure.

The results for smaller β values corresponding to real experimental situations show that the influence of stretching may be safely neglected for the trial Cantor set. It is, however, obvious that the experimental determination of the scaling indices is a more difficult task, in part because of the experimental noise and also because the slopes of the scaling dependences are not known *a priori*. This problem can be illustrated using data for the stretched Cantor set in Fig. 6. Indeed, if the data were corrupted with a noise that blurred scaling, this would lead to selection of a longer scaling interval and, therefore, overestimation of the scaling indices. However, the uncertainty is not crucial. This is demonstrated in Fig. 7 by taking an extremely high value of $\beta=10$. In this case, the slopes of the scaling dependences could not be determined correctly and the singularity spectrum became narrower. The correction was however quite low. In particular, it reached the value of 0.04 for $\alpha_{\min}$, which is small in comparison with the meaningful changes observed experimentally upon variation of the strain rate.

V. CONCLUSIONS

The undertaken investigations touched upon a general problem of determination of the structure of a noise, the intensity of which varies during an experiment. The plastic flow instability gives a simple example of such a situation. Indeed, the stress jump size and frequency may evolve with the material strain hardening reflecting the micrtostructure evolution. This gives rise to two interconnected problems: determine whether the dynamical structure of a signal remains the same and analyze it.

In the present paper, the example of the Portevin-Le Châtelier effect was used to prove the applicability of the multifractal technique to the study of collective dislocation processes showing up as macroscopic discontinuities on deformation curves. Comparison of multifractal spectra for the original and reconstructed deformation curves proved that the smooth trends in the stress serration parameters only lead to a contraction of the range of the scale invariant behavior but do not influence on the values of scaling indices and, therefore, do not prevent from evaluating the deterministic structure of the serrations. Herewith, the robustness of the multifractal analysis permits one either to avoid the unnecessary pretreatment of deformation curves or to justify a certain reconstruction procedure aimed at extending the scaling interval used for estimates.

In summary, the present data validate application of the multifractal analysis to the characterization of the complex structure of stress serrations, which reflect the collective dislocation dynamics, and detection of the changes that occur in the process of deformation or are induced by variation of experimental conditions. Together with the verification of the robustness of the multifractal structure with respect to random noise [13], it provides new evidences substantiating the multifractal concept for the study of the plastic instability and contiguous problems.

ACKNOWLEDGMENTS

The authors would like to thank A. Jacques for fruitful discussions. This work was partly supported by the Russian Foundation for Basic Research through Grant No. 04-02-17140. M.L. acknowledges support from CNRS for a one year stay at LPM.

[1] L. P. Kubin, C. Fressengeas, and G. Ananthakrishna, in *Dislocations in Solids*, edited by F. R. N. Nabarro and M. S. Duesbery (Elsevier Science BV, Amsterdam, 2002), Vol. 11, p. 101.
[2] Y. Estrin and L. P. Kubin, Mater. Sci. Eng., A **137**, 125 (1991).
[3] M. A. Lebyodkin, Y. Bréchet, Y. Estrin, and L. P. Kubin, Phys. Rev. Lett. **74**, 4758 (1995); Acta Mater. **44**, 4531 (1996).
[4] G. Ananthakrishna, C. Fressengeas, M. Grosbras, J. Vergnol, C. Engelke, J. Plessing, H. Neuhauser, E. Bouchaud, J. Plane's, and L. P. Kubin, Scr. Metall. Mater. **32**, 1731 (1995).
[5] S. Venkadesan, K. P. N. Murthy, S. Rajasekhar, and M. C. Valsakumar, Phys. Rev. E **54**, 611 (1996).
[6] S. J. Noronha, G. Ananthakrishna, L. Quaouire, C. Fressengeas, and L. P. Kubin, Int. J. Bifurcation Chaos Appl. Sci. Eng. **7**, 2577 (1997).
[7] M. A. Lebyodkin and L. R. Dunin-Barkovskii, Zh. Eksp. Teor. Fiz. **113**, 1816 (1998) [JETP **86**, 993 (1998)].
[8] G. Ananthakrishna, S. J. Noronha, C. Fressengeas, and L. P. Kubin, Phys. Rev. E **60**, 5455 (1999).
[9] M. Lebyodkin, L. Dunin-Barkowskii, Y. Bréchet, Y. Estrin, and L. P. Kubin, Acta Mater. **48**, 2529 (2000).
[10] G. D'Anna and F. Nori, Phys. Rev. Lett. **85**, 4096 (2000).
[11] M. S. Bharathi, M. Lebyodkin, G. Ananthakrishna, C. Fressengeas, and L. P. Kubin, Phys. Rev. Lett. **87**, 165508 (2001); M. S. Bharathi, M. Lebyodkin, G. Ananthakrishna, C. Fressengeas, and L. P. Kubin, Acta Mater. **50**, 2813 (2002).
[12] D. Kugiumtzis, A. Kehagias, E. C. Aifantis, and H. Neuhäuser, Phys. Rev. E **70**, 036110 (2004).
[13] M. A. Lebyodkin and Y. Estrin, Acta Mater. **53**, 3403 (2005).
[14] P. Barat, A. Sarkar, P. Mukherjee, and S. K. Bandyopadhyay, Phys. Rev. Lett. **94**, 055502 (2005).
[15] A. Portevin and F. Le Chatelier, Acad. Sci., Paris, C. R. **176**, 507 (1923).
[16] P. Bergé, Y. Pomeau, and C. Vidal, *Order within Chaos, towards a Deterministic Approach to Turbulence* (Wiley, New York, 1984).
[17] P. Bak, C. Tang, and K. Wiesenfeld, Phys. Rev. A **38**, 364 (1988).
[18] V. S. Bobrov, S. I. Zaitsev, and M. A. Lebyodkin, Fiz. Tverd. Tela (Leningrad) **32**, 3060 (1990) [Sov. Phys. Solid State **32**, 1176 (1990)].
[19] M. A. Lebyodkin, V. Ya. Kravchenko, and V. S. Bobrov, Physica B **165&166**, 267 (1990); Mater. Sci. Eng., A **164**, 252 (1993).
[20] M. A. Lebyodkin, L. R. Dunin-Barkovskii, V. S. Bobrov, and V. Gröger, Scr. Metall. Mater. **33**, 773 (1995); M. A. Lebyodkin, L. R. Dunin-Barkowskii, and T. A. Lebedkina, Pis'ma Zh. Eksp. Teor. Fiz. **76**, 714 (2002) [JETP **76**, 612 (2002)].
[21] M. C. Miguel, A. Vespignani, S. Zapperi, J. Weiss, and J. R. Grasso, Mater. Sci. Eng., A **309-310**, 324 (2001); **309-310**, 360 (2001).
[22] T. C. Halsey, M. H. Jensen, L. P. Kadanoff, I. Procaccia, and B. I. Shraiman, Phys. Rev. A **33**, 1141 (1986).
[23] P. W. Anderson, Phys. Rev. **109**, 1492 (1958).
[24] A. A. Andronov, A. A. Vitt, and S. E. Khaikin, *Theory of Oscillators* (Pergamon, Oxford, 1966).
[25] E. Pink, P. Bruckbauer, and H. Weinhandl, Scr. Mater. **38**, 945 (1998).
[26] J. Feder, *Fractals* (Plenum, New York, 1988).
[27] J. Mach, F. Mas, and F. Sague's, J. Phys. A **28**, 5607 (1995).
[28] A. Chhabra and R. V. Jensen, Phys. Rev. Lett. **62**, 1327 (1989).
[29] O. Malcai, D. A. Lidar, O. Biham, and D. Avnir, Phys. Rev. E **56**, 2817 (1997).
[30] E. Rizzi and P. Hähner, Int. J. Plast. **20**, 121 (2004).